The Journal of Immunology

Functional Transient Receptor Potential Melastatin 7 Channels Are Critical for Human Mast Cell Survival

Rob C. E. Wykes, Moonhee Lee, S. Mark Duffy, Weidong Yang, Elizabeth P. Seward and Peter Bradding

J Immunol 2007; 179:4045-4052; ;
doi: 10.4049/jimmunol.179.6.4045
http://www.jimmunol.org/content/179/6/4045

The Journal of Immunology is published twice each month by
The American Association of Immunologists, Inc.,
1451 Rockville Pike, Suite 650, Rockville, MD 20852

Print ISSN: 0022-1767 Online ISSN: 1550-6606.

Functional Transient Receptor Potential Melastatin 7 Channels Are Critical for Human Mast Cell Survival

Rob C. E. Wykes,[1]*† Moonhee Lee,† S. Mark Duffy,* Weidong Yang,* Elizabeth P. Seward,[2,3]† and Peter Bradding[2]*

Mast cells play a significant role in the pathophysiology of many diverse diseases such as asthma and pulmonary fibrosis. Ca^{2+} influx is essential for mast cell degranulation and release of proinflammatory mediators, while Mg^{2+} plays an important role in cellular homeostasis. The channels supporting divalent cation influx in human mast cells have not been identified, but candidate channels include the transient receptor potential melastatin (TRPM) family. In this study, we have investigated TRPM7 expression and function in primary human lung mast cells (HLMCs) and in the human mast cell lines LAD2 and HMC-1, using RT-PCR, patch clamp electrophysiology, and RNA interference. Whole cell voltage-clamp recordings revealed a nonselective cation current that activated spontaneously following loss of intracellular Mg^{2+}. The current had a nonlinear current-voltage relationship with the characteristic steep outward rectification associated with TRPM7 channels. Reducing external divalent concentration from 3 to 0.3 mM dramatically increased the size of the outward current, whereas the current was markedly inhibited by elevated intracellular Mg^{2+} (6 mM). Ion substitution experiments revealed cation selectivity and Ca^{2+} permeability. RT-PCR confirmed the presence of mRNA for TRPM7 in HLMC, LAD2, and HMC-1 cells. Adenoviral-mediated knockdown of TRPM7 in HLMC with short hairpin RNA and in HMC-1 with short interfering RNA markedly reduced TRPM7 currents and induced cell death, an effect that was not rescued by raising extracellular Mg^{2+}. In summary, HLMC and human mast cell lines express the nonselective cation channel TRPM7 whose presence is essential for cell survival. ***The Journal of Immunology,*** **2007, 179: 4045–4052.**

Mast cells are granulated tissue-dwelling leukocytes that form an important component of the innate immune system. Although they are best known for their role in allergy courtesy of their activation through the high-affinity IgE receptor by allergen, they have a critical role in tissue homeostasis, host defense, and the pathophysiology of many diverse diseases (1, 2). They orchestrate these processes through the release of numerous autacoid mediators, proteases and cytokines, for which differential release is dependent upon the stimulus (3).

Many cell processes, including cell proliferation, survival, chemotaxis, and activation for mediator release have an essential requirement for signals delivered by Ca^{2+} and Mg^{2+} (4, 5). Activation of mast cells by allergen for example has a critical dependence on the influx of Ca^{2+} from the extracellular space (6). Thus intracellular Ca^{2+} signals are often tightly coupled to ion channels in the plasma membrane that permit Ca^{2+} influx, and such Ca^{2+} channels are therefore attractive therapeutic targets. However, the molecular identities of the divalent cation influx pathways in human mast cells are unknown. Rodent mast cells demonstrate evidence of Ca^{2+} influx through both nonselective cation channels and store-operated Ca^{2+} channels (7, 8). The latter is carried by the CRACM1 (also known as Orai1) channel (9–12). Ca^{2+} currents and the channels carrying them in human mast cells are yet to be identified, although a human mast cell line opens a nonselective cation current following exposure to tamoxifen (13).

Potential candidates mediating mast cell cation influx are the transient receptor potential (TRP)[4] family of channels (14). TRP channels are classified by their homology, rather than function or selectivity. Channels from three main TRP protein subfamilies have been implicated in Ca^{2+} signaling, including members of the TRP melastatin (TRPM), TRP vanilloid (TRPV), and TRP canonical subfamilies. A survey of expression studies reveals that most tissues express mRNA for a multitude of TRP channels, including the lung. Using high-density oligonucleotide probe arrays, we previously identified the expression of TRP canonical-1 in human skin mast cells; TRPM2 in human skin, human cord blood, and human lung mast cells (HLMC); and TRPV2 in HLMC and human cord blood-derived mast cells but not human skin mast cells (15). Another TRP family member not examined in this original gene array study was TRPM7. This channel is widely expressed and carries divalent cations including Ca^{2+} and Mg^{2+}, and it has been identified in the rat mast cell line RBL-2H3 and Jurkat T cells (16). The function of TRPM7 remains poorly understood, but there is evidence that it is involved in Mg^{2+} homeostasis and can carry numerous trace divalent cations essential to normal human health (17). TRPM7 activity is regulated by intracellular concentrations of Mg^{2+} and $Mg^{2+} \cdot ATP$, with increasing concentrations inhibiting its gating. It is an unusual channel in that it expresses an α-kinase in its N terminus. This enzyme is not essential for channel

*Department of Infection, Immunity and Inflammation, Institute for Lung Health, University of Leicester, Leicester, United Kingdom; and †Department of Biomedical Science, University of Sheffield, Western Bank, Sheffield, United Kingdom

Received for publication June 22, 2007. Accepted for publication June 30, 2007.

The costs of publication of this article were defrayed in part by the payment of page charges. This article must therefore be hereby marked *advertisement* in accordance with 18 U.S.C. Section 1734 solely to indicate this fact.

[1] Current address: Department of Physiology M211, Northwestern University, 303 East Chicago Avenue, Chicago, IL 60611.

[2] E.P.S. and P.B. are joint senior authors for this work.

[3] Address correspondence and reprint requests to Dr. Elizabeth P. Seward, Department of Biomedical Science, Alfred Denny Building, University of Sheffield, Western Bank, Sheffield S10 2TN, U.K. E-mail address: e.p.seward@sheffield.ac.uk

[4] Abbreviations used in this paper: TRP, transient receptor potential; TRPM, TRP melastatin; TRPV, TRP vanilloid; HLMC, human lung mast cell; siRNA, short interfering RNA; shRNA, short hairpin RNA; eGFP, enhanced GFP; $[Ca^{2+}]_i$, intracellular Ca^{2+} concentration; Vm, reversal potential; I_{CRAC}, Ca^{2+} release-activated Ca^{2+} current.

gating but has been shown to phosphorylate annexin I and actomyosin and thus couples the channel to the cytoskeleton (18, 19). Channel knockdown has been shown to induce cell death (16), inhibit cell proliferation (20), and inhibit or enhance cell adhesion depending on the model studied (18, 19).

In this study we have investigated TRPM7 expression and function in human mast cells using a combination of RT-PCR, patch clamp electrophysiology, and RNA interference. We demonstrate for the first time that human mast cells express functional TRPM7 channels whose presence is essential for cell survival.

Materials and Methods

Reagents

We used the following reagents: stem cell factor, IL-6, and IL-10 (R&D Systems); mouse IgG1 mAb YB5B8 (anti-CD117; Cambridge Bioscience); sheep anti-mouse IgG1 Dynabeads (Dynal Biotech); DMEM/Glutamax/HEPES, antibiotic/antimycotic solution, MEM nonessential amino acids, and FCS (Invitrogen Life Technologies); HiPerfect transfection reagent (Qiagen); TRPM7 short interfering RNA (siRNA) and controls (Invitrogen Life Technologies); TRPM7 short hairpin RNA (shRNA) and controls (Biofocus). Physiological salts were purchased from Sigma-Aldrich unless otherwise stated.

Human mast cells

HLMC were dispersed and purified from macroscopically normal lung obtained within 1 h of resection for lung cancer by using immunomagnetic affinity selection as previously described (21). Final mast cell purity was >99% with >97% viability. All human subjects gave written informed consent, and the study was approved by the Leicestershire Research Ethics Committee. HLMC were cultured in DMEM/Glutamax/HEPES containing antibiotic/antimycotic solution, nonessential amino acids, 10% FCS, 100 ng/ml stem cell factor, 50 ng/ml IL-6, and 10 ng/ml IL-10. Half the medium was replaced every 7 days.

LAD2 mast cells, derived from a patient with mast cell leukemia, were a gift from Dr. D. Metcalfe (National Institute of Allergy and Infectious Diseases, National Institutes of Health, Bethesda, MD) and cultured in StemPro-34 SFM serum-free complete medium (Invitrogen Life Technologies), with 100 ng/ml stem cell factor as previously described (22). Half the medium was replaced every 7 days.

The HMC-1 cell line, derived from a patient with mast cell leukemia, was a gift from Dr. J. Butterfield (Mayo Clinic, Rochester, MN). HMC-1 cells were maintained in Iscove's modified DMEM (Invitrogen Life Technologies) as previously described (23).

RT-PCR

RNA was prepared from cell lysates (Qiagen) and 500 ng converted to cDNA (BioRad iScript kit). With the aid of the Primer 3 program, PCR primers specific for human TRPM6 and TRPM7 were designed to span across exons to avoid possible amplification of genomic DNA. All primers were checked for specificity using a BLAST search of the human genome. The following two pairs of primers were used for each channel: TRPM7 5′-TGAAACGAGTGAGTTCTCTTGCTG and 3′-CACAGGTGTAAATG GAATGCTC, predicted product band size 309 bp, or 5′-TGGCATATGA AGCAAAGCAG and 3′-AGCAATATGGCAGGTGGAAC, predicted product size 334 bp; TRPM6 5′-TTATGATTGGCACCTGGAGTCCTTG and 3′-TGATTCCTCTCGGAGTGAACAGCAC, predicted band size of 347 bp, or 5′-CCAGAGCCAGGAGAAAACAG and 3′-AAAGGGGAAC TCTCCTCCAA, predicted product band size 419 bp. RT-PCR was performed (35 cycles of amplification) using a Thermo-Start PCR master mix (ABgene), with each cycle consisting of 94°C for 30 s, 56°C for 30 s, and 72°C for 30 s. RT-PCR for β-actin was performed as a positive control, and for TRPV2 (5′-GGCTGGCTGAACCTGCTTTAC and 3′-TGGCGACA CTGTTGACGGTCTC, product size 445 bp) as an internal control for TRPM7 siRNA knockdown experiments (see below).

Electrophysiology

Mast cells adherent to 0.01% poly-L-lysine-coated coverslips were placed in a microperfusion chamber and viewed under an inverted phase-contrast microscope (Zeiss Axiovert 25 or 100). Cells were continuously superfused at a high flow rate (>2 ml/min) with an external solution containing the following: 147 mM NaCl, 2 mM KCl, 1 mM $MgCl_2$, 2 mM $CaCl_2$, 13 mM glucose, 10 mM HEPES (pH adjusted to 7.3) with sodium hydroxide; osmolarity adjusted with sucrose to ~310 mOsm. Currents were recorded in the whole cell patch configuration using borosilicate glass electrode coated with Sylgard 184 (Dow Corning) and fire polished on a microforge to a resistance of 3–4 MOhm. Initial experiments used a basic pipette recording solution containing 147 mM NaCl, 10 mM HEPES, and 10 mM EGTA. In subsequent experiments pipettes were filled with internal solution containing 135 mM cesium-glutamate, 8 mM NaCl, 10 mM HEPES, 10 mM EGTA, 3.6 mM $CaCl_2$ (adjusted to pH 7.3 with cesium hydroxide (ICN Biomedicals)); osmolarity ~305 mOsm. This recording solution buffers intracellular Ca^{2+} to ~100 nM (calculated using WEBMAXCLITE v.1.15, available at www.stanford.edu/~cpatton/webmax). A liquid junction potential of −13 mV was corrected for offline. Series resistance was usually <10 MOhm, and never higher than 17 MOhm. Series resistance was also compensated (typically >70%) electronically using a patch clamp amplifier (Axopatch 200B; Axon Instruments). Voltage protocol generation and data acquisition were performed using the pClamp program (v.6), running on a Pentium computer equipped with a Digidata acquisition board (Axon Instruments). 200 ms ramps from −100 to +100 mV were evoked from a membrane holding potential of 0 mV. Current traces were low-pass filtered at 5 kHz using a four-pole Bessel filter supplied with the amplifier and digitized at 10 kHz. Data were stored on the computer hard drive and analyzed offline using commercial software (Origin; Microcal).

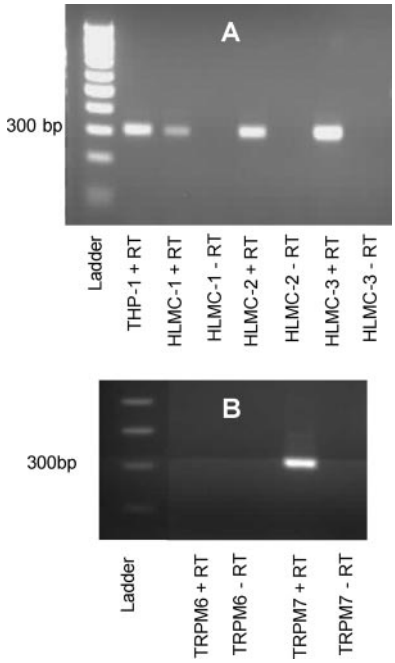

FIGURE 1. RT-PCR confirms the expression of mRNA for TRPM7 but not for TRPM6. *A*, Gels demonstrating expression of TRPM7 in three HLMC donors (THP-1 cells were used as a positive control at a predicted band size 309 bp). *B*, Gel expression of TRPM7 but not TRPM6 in LAD2 cells. The same results were observed when different TRPM6 and TRPM7 primers were used (data not shown).

RNA interference

HMC-1 cells were transfected according to the manufacturer's instructions using HiPerFect transfection reagent, with one of three following pairs of TRPM7 siRNA oligonucleotides: TRPM7A 5′-AAACGAUACACUG UGACAGGCUCCC and 3′-GGGAGCCUGUCACAGUGUAUCGUUU; TRPM7B 5′-AAUACUUGACCAUGUAUUAACCACC and 3′-GGUGG UUAAUACAUGGUCAAGUAUU; and TRPM7C 5′-AACAUCAGACG AACAGAAUUAGUUG and 3′-CAACUAAUUCUGUUCGUCUGAUG UU), a control scrambled oligonucleotide, and a FITC-labeled control oligonucleotide. For RT-PCR, cells were lysed 48 h later and RNA extracted. A total of 500 ng of total RNA per sample was converted to cDNA and used for RT-PCR experiments (30 cycles of amplification) to determine relative TRPM7 mRNA expression. The PCR band intensity was derived using densitometry (GeneGenius; Bio-Imaging Technologies). Cell survival was monitored using trypan blue dye exclusion and cells counted on a hemocytometer (Sigma-Aldrich).

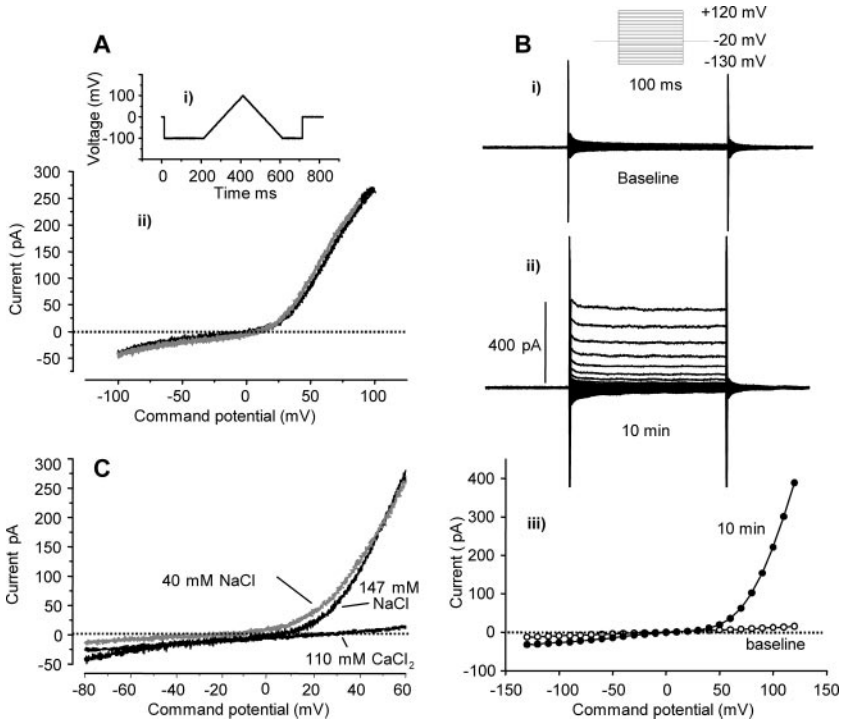

FIGURE 2. An outwardly rectifying, cation-selective current develops slowly after obtaining the whole cell configuration. *A*, Schematic showing current-voltage (I-V) curves were generated by applying 200 ms voltage ramps from a holding potential of 0 mV (i). A 200-ms conditioning pulse to −100 mV was applied before the ramp to allow inactivation to reach a quasi-steady state preventing distortion of the I-V curve by inactivation during the ramp. Currents evoked by a ramp (ii) from −100 to +100 mV (black line) mirrored the resultant current evoked by the ramp back from +100 to −100 mV (gray line), indicating good voltage clamp and no current inactivation during the ramp. *B*, A second voltage protocol was also routinely used. From a holding potential of −20 mV, single steps of 100-ms duration were applied in 10-mV increments (−130 to +120 mV) (*inset*). Immediately after obtaining the whole cell configuration (baseline), no current is evident (i). Using this protocol, a similar outwardly rectifying current developed over time (ii). This current displayed no notable inactivation over the duration of the pulse and developed slowly with peak current amplitudes recorded 7–10 min after obtaining the whole cell configuration (i vs ii). The amplitude of the current then remained stable for the duration of the experiments (20–30 min). I-V curve from the same cell is shown (iii). Results are from representative HLMCs. *C*, Ion substitution experiments were used to determine the ion selectivity of the current. Using a 3 M KCl agar bridge as a ground reference, the normal extracellular solution was replaced with one containing low sodium chloride (plus glucose to maintain isotonicity) or isotonic Ca^{2+}. The shifts in the currents Vm following solution exchange show that the current is cation selective (sodium chloride line) and calcium permeable (calcium chloride line). Results are from representative LAD2 cell experiments.

Adenoviral transfection and shRNA delivery in HLMC

Adenoviruses encoding enhanced GFP (eGFP) and shRNA directed against eGFP, luciferase, and three different target sequences for human TRPM7 (referred to as v1, v2 and v3) were purchased from Biofocus. The optimal protocol for transduction of primary HLMC was determined empirically by fluorescent imaging of cells 1–6 days after infection with the eGFP virus (Ad5C20Att01, titer $2.9E^{+10}$ vp/ml). HLMCs collected from three donors, were plated in triplicate in 100 μl of medium into each well of a 96-well plate (10^4 cells/well). A total of 50 μl of virus diluted to give a multiplicity of infection of 500, 1000, or 2000 was then added to the wells and the cells returned to the incubator until the time of experiment. Even at multiplicity of infection of 500, good (>70%) transduction of cells, as judged by the appearance of green fluorescence, was observed 3 days postinfection. For transduction with shRNA adenoviruses, cells were infected with multiplicity of infection of 2000. Nonspecific effects of adenoviral infection on cell viability and ion channel expression were assessed in time- and culture-matched experiments performed on cells infected with either the eGFP adenovirus or control shRNA targeted against eGFP and luciferase.

Data presentation and statistical analysis

Data are expressed as mean ± SEM unless otherwise stated. Differences between groups of data were explored using one-way ANOVA or Student's paired or unpaired *t* test (two-tailed) as appropriate.

Results

HLMC and mast cell lines express TRPM7 but not TRPM6 mRNA

Two closely related TRPM channel subtypes, TRPM6 and TRPM7, are activated by lowered intracellular Mg^{2+} and have similar biophysical properties including an outwardly rectifying current-voltage (I-V) relationship, cation selectivity P_{Na}/P_{Cl} = 1/0.06, and divalent permeability (24). To investigate whether one or both of these channels are expressed in HLMC, LAD2 cells, and HMC-1 cells, we performed RT-PCR experiments to determine the expression of mRNA for the two channels. We consistently observed strong expression for TRPM7 in HLMC (5/5 donors), LAD2 cells and HMC-1 cells (Fig. 1). In contrast, we could not detect expression of mRNA for TRPM6. This supports the observation that TRPM6 is expressed predominantly in the kidney and small intestine but not the lung (25, 26), and is consistent with the failure to detect expression of this channel by human mast cells from skin and lung in a previous gene array study (15).

Human mast cells express TRPM7-like currents

TRPM7 is known to be regulated by the concentration of intracellular Mg^{2+}, with strong current activation occurring when concentrations fall below 1 mM (16, 27). To investigate whether a TRPM7-like current could be activated in HLMC and a model human mast cell LAD2, we initially conducted electrophysiological experiments using a simplified pipette solution (symmetric sodium chloride), which contained no Mg^{2+}. Applying a 200 ms voltage ramp from −100 to +100 mV (Fig. 2*A*), we evoked a steeply outwardly rectifying current, with a reversal potential (Vm) of +5.2 ± 2.4 mV in LAD2 cells (n = 21) and 3.4 ± 0.4 mV in

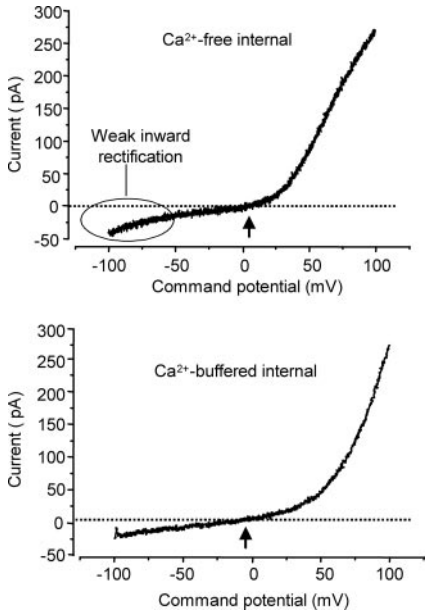

FIGURE 3. A Ca^{2+}-buffered internal solution prevents activation of an I_{CRAC}-like current. By using an intracellular pipette solution designed to prevent activation of I_{CRAC}, a small but nonsignificant change in mean inward currents was observed in both LAD2 cells and HLMCs, with loss of the weak inward rectification evident at negative command potentials. A small but significant ($p = 0.004$) leftward shift in the current reversal potential (arrows) was observed using the Ca^{2+}-buffered internal solution, suggesting a small contamination of the TRPM7-like current by an I_{CRAC}-like current. Data demonstrate examples from representative LAD2 cells.

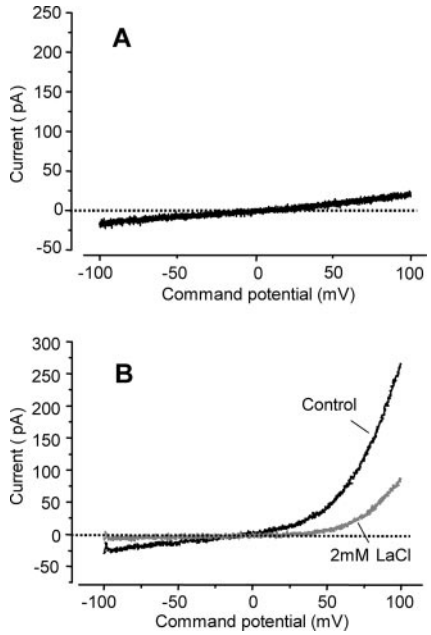

FIGURE 4. Current activation is suppressed by raised (6 mM) intracellular Mg^{2+} and inhibited by 2 mM external La^{3+}. *A*, Inclusion of 6 mM Mg^{2+} (a concentration known to suppress TRPM7 activation) in the pipette solution dramatically reduced current activation in HLMCs. Current activation was also inhibited in LAD2 cells (data not shown). *B*, La^{3+} (2 mM) completely blocked the inward but only partially blocks the outward currents of cloned TRPM7 channels. A total of 2 mM La^{3+} reduced both the inward and outward currents in HLMCs in a similar manner. The current was also inhibited to a similar extent in LAD2 cells (data not shown). Data demonstrate currents in representative HLMC.

HLMC ($n = 9$), indicating activation of either a nonselective cationic conductance or Cl^- conductance. Similar currents were obtained using voltage steps (Fig. 2*B*). This I-V curve is reminiscent of the current-voltage properties of several TRP channels including TRPM7 (16). The current developed slowly over time with peak current amplitudes occurring 7–10 min after obtaining the whole cell configuration (Fig. 2*B*), and remained stable for the duration of the experiments (20–30 min). This slow time course for current activation is compatible with the dialysis of a cytoplasmic regulator such as Mg^{2+} that suppresses current activation under resting conditions. The mean peak inward and outward currents for HLMC at -100 and $+100$ mV were -33.2 ± 5.8 pA and $+171.1 \pm 18.2$ pA, respectively ($n = 9$), and for LAD2 -42.7 ± 5.8 pA and $+152.4 \pm 17.4$ pA, respectively ($n = 21$). Reducing the external divalent cation concentration from 3 to 0.3 mM dramatically increased the size of the outward current; LAD2 mean inward peak current increased to -47.2 ± 6.8 pA and outward to $+352.4 \pm 55.7$ pA ($n = 11$, $p = 0.0002$). To investigate the ion selectivity of the current we performed ion substitution experiments. Replacement of the standard (147 mM NaCl) extracellular solution to one containing 40 mM NaCl resulted in a leftward shift in the current Vm from $+3.5 \pm 1.4$ mV to -25.7 ± 6.2 mV; $P_{Cl}/P_{Na} = 0.06/1$ ($n = 4$ LAD2 cells, $p = 0.0027$), indicating that the current carries cations rather than Cl^- (Fig. 2*C*). Switching to an external recording solution composed of 110 mM $CaCl_2$ resulted in a rightward shift in the Vm to $+15.2 \pm 4.3$ mV ($n = 4$ LAD2 cells, $p = 0.041$). This result, coupled with the increase in inward current in 110 mM $CaCl_2$ compared with 40 mM NaCl is indicative of Ca^{2+} permeability (Fig. 2*C*).

In the initial whole cell patch experiments described, we used a simplified pipette solution. Under these conditions resting intracellular Ca^{2+} concentration ($[Ca^{2+}]_i$) is decreased. It has previously been shown that simplified pipette solutions similar to these can activate both TRPM7 and the Ca^{2+} release-activated Ca^{2+} current (I_{CRAC}) (28, 29). We therefore examined whether $[Ca^{2+}]_i$ influenced the amplitude or biophysical characteristics of the recorded current. To examine this, we used a pipette solution designed to buffer $[Ca^{2+}]_i$ to 100 nM (see *Materials and Methods* for composition), which would allow us to determine whether our original TRPM7-like currents were contaminated by I_{CRAC}. I_{CRAC} displays an inwardly rectifying I-V curve with a positive Vm. The size of the mean inward currents in LAD2 cells and HLMC were not significantly different when the two pipette solutions were compared (Fig. 3). However, there was a small, but significant leftward shift in the Vm (no Ca^{2+} buffering Vm $+5.2 \pm 2.4$ mV, $n = 21$ LAD2 cells; 100 nM buffered Ca^{2+} Vm -3.5 ± 1.1 mV, $n = 17$ LAD2 cells; $p = 0.004$). Visual inspection of the traces revealed a slight inward rectification at negative potentials for currents recorded in Ca^{2+}-free internal solution, which was absent when Ca^{2+} was buffered to 100 nM (Fig. 3). This finding suggests that under our original recording solutions, there was a small contamination of the TRPM7-like current by another conductance, possibly I_{CRAC}. To avoid any further possible contamination of current traces by I_{CRAC}, subsequent experiments were conducted using the Ca^{2+}-buffered internal solution.

There are presently no specific blockers for TRPM7 commercially available but TRPM7 has been reported to be inhibited by raised (6–10 mM) concentrations of intracellular Mg^{2+} (16, 27, 28, 30). Inclusion of 6 mM Mg^{2+} in the patch pipette effectively blocked current activation in HLMC ($n = 7$ cells) (Fig. 4*A*). La^{3+} (2 mM) has been reported to completely block the inward, but only partially block the outward currents of cloned TRPM7 channels

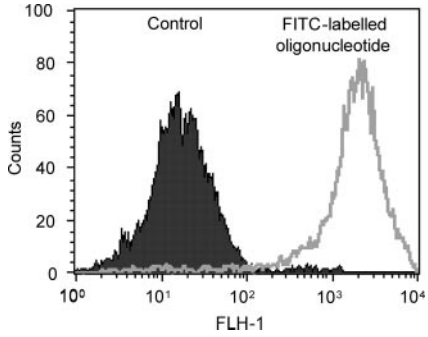

FIGURE 5. Uptake of a FITC-labeled oligonucleotide by the HMC-1 cell line as assessed by flow cytometry.

(31). We found that extracellular application of 2 mM La^{3+} reduced both the inward ($p = 0.012$) and outward ($p = 0.04$) currents in HLMC ($n = 4$) in a similar manner to those reported for the cloned channel (Fig. 4*B*).

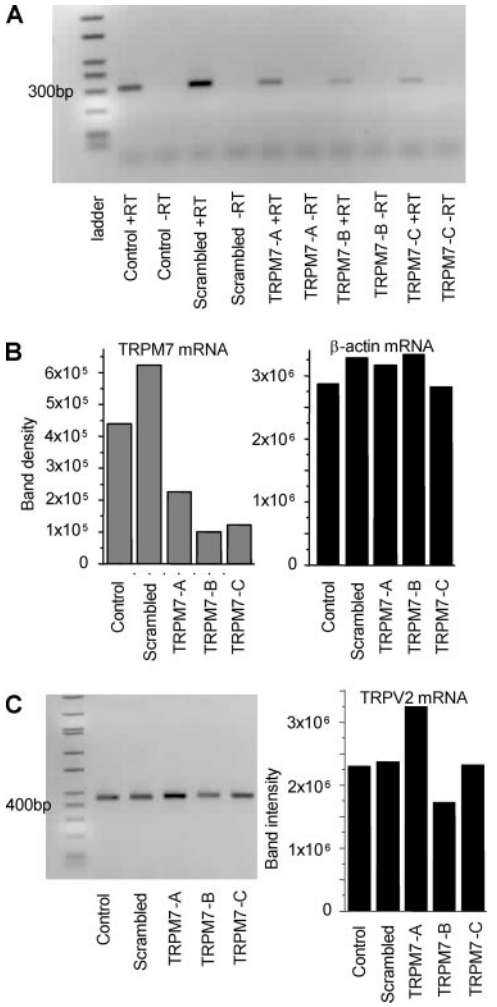

FIGURE 6. The siRNA-mediated knockdown of TRPM7 mRNA. *A*, Gel demonstrating reduced mRNA expression for TRPM7 in HMC-1 following transfection with three different TRPM7 siRNA oligonucleotides (A, B, and C). *B*, Quantification of the gel shown in *A* using densitometry. No knockdown of β-actin was seen. *C*, TRPV2 mRNA was not knocked down by TRPM7 siRNA constructs.

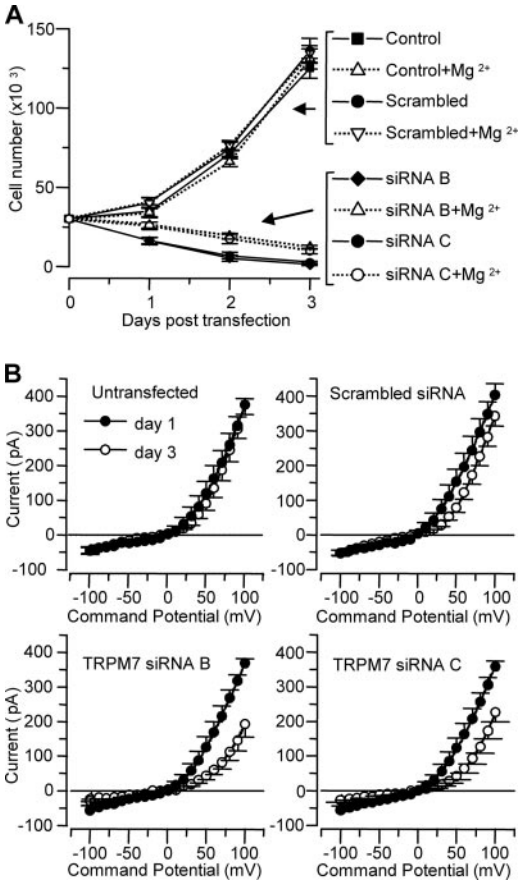

FIGURE 7. The siRNA-mediated reduction in TRPM7 currents and cell survival. *A*, TRPM7 siRNAs induced death of HMC-1 cells over a period of 72 h from transfection. This effect was not rescued significantly by 10 mM extracellular Mg^{2+}. Mean of three experiments performed on different occasions, each in triplicate is shown. $p < 0.001$ by ANOVA at days 1, 2, and 3. *B*, In viable cells, TRPM7 currents were markedly reduced at both 48 and 72 h by TRPM7 siRNA constructs but not a scrambled control siRNA. Mean data from two experiments performed on separate occasions ($n = 6$ cells per condition).

TRPM7 is not regulated by β_2-adrenoceptors in HLMC

TRPM7 currents are reported to be activated by the nonselective β-adrenoceptor agonist isoproterenol (32). However, TRPM7 currents in HLMC were not augmented or suppressed by either the selective β_2-adrenoceptor agonist salbutamol at concentrations up to 10^{-5} M ($n = 4$ cells, $p = 0.11$) or the selective β_2-adrenoceptor antagonist and inverse agonist ICI 118551 at concentrations up to 10^{-6} M ($n = 4$ cells, $p = 0.34$).

TRPM7 knockdown induces cell death in the HMC-1 human mast cell line

All the properties of the current reported in this study are comparable to those described for the cloned recombinantly expressed human TRPM7 channel (16, 31). For conclusive proof that the current was mediated by activation of TRPM7, we first performed siRNA experiments in HMC-1 to knock down mRNA expression and therefore, consequently, protein expression of TRPM7. We used three different siRNA oligonucleotides designed against the TRPM7 mRNA sequence (TRPM7 A, B, and C). In preliminary experiments using a FITC-labeled oligonucleotide and flow cytometry, we assessed the transfection efficiency in HMC-1 cells to be 95% (Fig. 5). RT-PCR showed that transfection of each of the TRPM7 siRNA constructs resulted in a significant reduction in

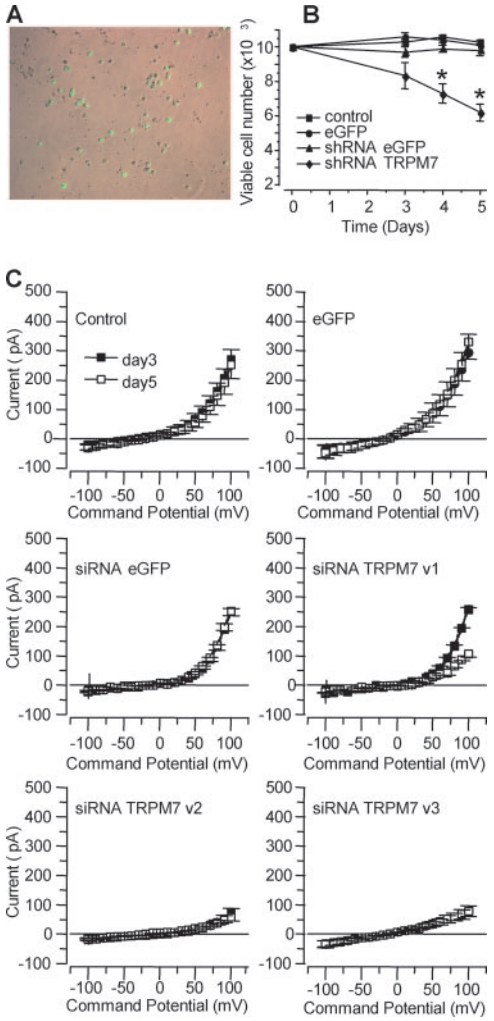

FIGURE 8. The shRNA-mediated reduction in TRPM7 currents and HLMC survival. *A*, Transfection of primary HLMC with the Ad5C20Att01 adenovirus containing an eGFP construct reveals >70% transfection efficiency. Brightfield image is overlaid with fluorescent imaging at magnification of ×100. *B*, Adenoviral transduction of HLMC with shRNA to TRPM7 reduces cell survival, but shRNA to GFP and overexpressed eGFP have no effect on cell viability. Mean of three experiments performed on HLMC from two donors is shown. **, $p < 0.05$ compared with control. *C*, Adenoviral transfection of HLMC with shRNA to TRPM7 reduces the size of the TRPM7 currents in three different target sequences for human TRPM7 (referred to as v1, v2, and v3). Mean data from two HLMC donors for TRPM7 v2 and v3 ($n = 6$ cells per condition), and from a separate HLMC donor for TRPM7 v1 ($n = 3$ cells per condition). There was no change in the size of the currents under control conditions.

mRNA expression for TRPM7 (Fig. 6, *A* and *B*) without reducing the expression of either β-actin or another related TRP channel (TRPV2) (Fig. 6*C*). The TRPM7 siRNA B and C were most effective and were used for additional experiments.

Monitoring cell survival using trypan blue demonstrated that HMC-1 cells transfected with a control scrambled siRNA continued to proliferate rapidly (Fig. 7*A*). In contrast, there was rapid cell death in cells transfected with TRPM7 siRNA B and C, so that after 3 days nearly all cells had died ($p < 0.001$ by ANOVA) (Fig. 7*A*). There was only marginal rescue by culturing HMC-1 in 10 mM extracellular Mg^{2+} (Fig. 7*A*), which was not significant when applying a *t* test with Bonferroni's correction for multiple comparisons.

To confirm that the siRNAs had reduced TRPM7 protein expression, cells were also analyzed using electrophysiology. Cells that had been cotransfected with a FITC-labeled oligonucleotide were identified and recorded 24, 48, and 72 h after transfection. This analysis was complicated by the fact that TRPM7 knockdown killed the cells, but nevertheless it was possible to demonstrate in remaining viable cells at 48 and 72 h, that TRPM7 siRNA B and C significantly reduced the magnitude of TRPM7 currents when compared with the scrambled control (Fig. 7*B*). Thus at +100 mV, outward current was 324 ± 27.4 pA in scrambled controls at 72 h posttransfection, compared with 188 ± 37.1 pA for TRPM7 siRNA B ($p = 0.016$) and 223 ± 28.5 pA ($p = 0.032$) for TRPM7 siRNA C ($n = 6$ cells for each condition). Transfection with the scrambled siRNA control had no effect on TRPM7 currents ($p = 0.26$) (Fig. 7*B*).

TRPM7 knockdown induces cell death in primary HLMC

Efficient transfection of HLMC to date has not been possible using lipid transfection reagents (our unpublished data). We therefore used an adenoviral delivery system for the transduction of primary HLMC. Using eGFP as a control, we were able to demonstrate >70% transduction efficiency without loss of cell viability (Fig. 8*A*). We tested the ability of adenoviruses expressing three different shRNA constructs targeted at TRPM7 (v1, v2, and v3) to knock down TRPM7 currents in HLMC from three different donors. Transfection with two irrelevant shRNA constructs targeted at eGFP and luciferase, and with eGFP itself, did not alter cell viability or the magnitude of the TRPM7 currents (Fig. 8, *B* and *C*). In contrast infection with adenovirus engineered to express shRNA TRPM7 v1, v2, and v3 all reduced cell viability from days 3–5 postinfection, with v2 and v3 being the most effective (Fig. 8*B*) ($p < 0.05$ for combined TRPM7 shRNA compared with culture-matched controls at both days 4 and 5; $n = 3$ experiments performed on HLMC from two donors). In viable cells, TRPM7 currents were markedly reduced by shRNA TRPM7 v2 and v3 by 3 days after infection and by 5 days after infection with v1 (Fig. 8*C*). Thus at +100 mV, outward current was 248 ± 29.7 pA in control cells ($n = 9$) 5 days posttransfection, compared with 58.9 ± 11.5 pA for TRPM7 v2 ($p = 0.0004$, $n = 6$), and 79.7 ± 18.3 pA for TRPM7 v3 ($p = 0.0004$, $n = 6$). Currents were also reduced by adenovirus carrying shRNA TRPM7 v1 but less markedly (current at +100 mV 107.3 ± 9.2 pA, $p = 0.001$, $n = 3$).

Discussion

We have identified molecularly the first functionally active cation channel in HLMC and human mast cell lines capable of carrying divalent cations. The biophysical properties of this channel indicate it is TRPM7, which is supported by the expression of TRPM7 mRNA in these cells, and loss of current activity after "knockdown" using TRPM7 RNA interference. Knockdown was highly effective and lead to cell death, indicating an essential role for this channel in cell survival.

TRPM7 is a member of the melastatin-like subfamily of transient receptor potential ion channels. It is very closely related to TRPM6 with which it shares very similar electrophysiological properties and an α-kinase domain in the C terminus. Although both channels are apparently involved in Mg^{2+} homeostasis, and can potentially form TRPM6/7 heterodimers, they have also been shown to have nonredundant roles (33). In this study we did not see expression of TRPM6 using RT-PCR, and it was not expressed in human mast cells from skin, lung, or cord blood when analyzed by DNA microarrays (15). Furthermore expression of TRPM6 is localized predominantly to the kidney and small intestine, and is absent in several tissues in which mast cells are present (25, 26).

Taken together, this result suggests that the current we have identified is carried only by TRPM7.

We have previously identified several ion channels and currents in human mast cells but had not previously identified TRPM7 because we had always performed electrophysiological recordings with intracellular Mg^{2+} and ATP present, which inhibit the channel (13, 23, 34–36). The electrophysiological properties of the currents recorded in this study are identical with those previously described for cloned heterologously expressed TRPM7 (16, 31). Furthermore, siRNA knockdown of TRPM7 in HMC-1 was associated with both reduced TRPM7 mRNA expression and ionic currents. This property was specific for TRPM7 in that there was no knockdown of TRPM7 with a scrambled siRNA control, and no knockdown of TRPV2 mRNA with the TRPM7 siRNA. Similarly, three distinct adenoviral-delivered shRNA, which target TRPM7, reduced the magnitude of TRPM7 currents in HLMC, whereas several controls did not. Thus we have used several approaches, which when taken together, confirm that the channel we have identified in HMC-1 cells, LAD2 cells, and HLMC is indeed TRPM7.

The presence of functional TRPM7 has been reported to be a critical requirement for cell survival in several model systems. Therefore it is perhaps not surprising that its knockdown also lead to cell death of the HMC-1 human mast cell line and primary HLMC. The mechanism by which TRPM7 maintains cell survival in DT-40 chicken B cells has been proposed to be through its ability to maintain Mg^{2+} homeostasis because the lethal effects of TRPM7 knockdown can be rescued by raising the extracellular concentration of Mg^{2+} (16). However, high extracellular Mg^{2+} did not prevent cell death in retinoblastoma cell lines following TRPM7 knockdown (20), and we found it only had a minimal effect on rescuing HMC-1 mast cells. This effect might be because unlike DT-40 cells, HMC-1 cells, and retinoblastoma have no other Mg^{2+} entry pathways, such as the closely related TRPM6, or Mg^{2+} transporters such as SLC41A2 family proteins (37), which may compensate for the loss of TRPM7 channel and maintain Mg^{2+} at sufficient levels for the cells to survive. Interestingly, the α-kinase domain of TRPM7 phophorylates annexin I (38), and because annexin I is itself implicated in the regulation of cell growth, differentiation, and apoptosis (39, 40), this finding may provide another link between TRPM7 and cell survival.

Examining the further physiological roles of TRPM7 in mast cells will be difficult because the cells die rapidly. However, it seems likely that the role of TRPM7 extends beyond maintaining cell survival and divalent cation homeostasis. The α-kinase domain in the TRPM7 C terminus phosphorylates actomyosin and interferes with cell adhesion and spreading (18, 19). However, there are contradictory studies detailing whether cell spreading is enhanced or diminished following TRPM7 knockdown (18, 19). Nevertheless, this finding suggests that TRPM7 may play an important role in cell migration and cell-cell interactions. TRPM7 has also been shown to contribute to intracellular Ca^{2+} signals in retinoblastoma cells (20). Thus retinoblastoma cells over-expressing TRPM7 demonstrated elevated baseline cytosolic-free Ca^{2+}, and enhanced Ca^{2+} influx following stimulation with bradykinin. If applicable to other cell types such as mast cells, TRPM7 could potentially contribute to the Ca^{2+} signal of various cell responses such as Ag-induced secretion and migration, and growth factor-dependent cell survival.

Takezawa et al. (32) reported that the TRPM7 channel is regulated by β-adrenoceptors even in the presence of 3 mM intracellular $Mg^{2+} \cdot$ ATP as demonstrated by the application of the non-selective β-agonist isoproterenol at high concentrations (320 μM). This report is in contrast to our previous experience in HLMC with the selective β_2-adrenoceptor agonist salbutamol (36). We have shown previously that salbutamol closes the intermediate conductance Ca^{2+}-activated channel $K_{Ca}3.1$ in HLMC, whereas the selective β_2-adrenoceptor inverse agonist ICI 118551 opens it. Whether recording in either the whole cell or perforated patch mode of the patch clamp technique, we never saw the development of a TRPM7 current in response to salbutamol (36). In this study we have extended this work to look at the effects of salbutamol on TRPM7 currents, which had been activated in the absence of intracellular Mg^{2+} and ATP. Again, salbutamol and ICI 118551 were without effect. Thus we conclude that β_2-adrenoceptors are not coupled to TRPM7 in HLMC.

Previous attempts to transfect primary HLMC with plasmids using numerous lipid transfection reagents have failed (our unpublished data). We now show that the Ad5C20Att01 adenovirus is highly efficacious at carrying plasmids into HLMC and for the delivery of shRNA. Also, for up to 5 days this virus does not alter cell viability. This technique is therefore an invaluable tool for studying the biology of primary HLMC and will permit the genetic manipulation of many intracellular signaling pathways.

In summary we have demonstrated that human mast cells express functional TRPM7 channels that are a critical requirement for cell survival. This requirement of functional channels for cell survival means it may prove difficult to determine the further biological roles of this interesting channel in human mast cells. Nevertheless, identifying mast cell-specific regulatory pathways for TRPM7 may offer novel approaches to modifying mast cell function in a variety of diseases.

Disclosures

The authors have no financial conflict of interest.

References

1. Bradding, P., and S. T. Holgate. 1999. Immunopathology and human mast cell cytokines. *Crit. Rev. Oncol. Hematol.* 31: 119–133.
2. Bradding, P., A. F. Walls, and S. T. Holgate. 2006. The role of the mast cell in the pathophysiology of asthma. *J. Allergy Clin. Immunol.* 117: 1277–1284.
3. Okumura, S., J. Kashiwakura, H. Tomita, K. Matsumoto, T. Nakajima, H. Saito, and Y. Okayama. 2003. Identification of specific gene expression profiles in human mast cells mediated by TLR4 and FcεRI. *Blood* 102: 2547–2554.
4. Berridge, M. J., P. Lipp, and M. D. Bootman. 2000. The versatility and universality of calcium signaling. *Nat. Rev. Mol. Cell Biol.* 1: 11–21.
5. Romani, A. M., and A. Scarpa. 2000. Regulation of cellular magnesium. *Front. Biosci.* 5: D720–D734.
6. Caulfield, J. P., R. A. Lewis, A. Hein, and K. F. Austen. 1980. Secretion in dissociated human pulmonary mast cells: evidence for solubilization of granule contents before discharge. *J. Cell Biol.* 85: 299–312.
7. Hoth, M., and R. Penner. 1992. Depletion of intracellular calcium stores activates a calcium current in mast cells. *Nature* 355: 353–356.
8. Fasolato, C., M. Hoth, G. Matthews, and R. Penner. 1993. Ca^{2+} and Mn^{2+} influx through receptor-mediated activation of nonspecific cation channels in mast cells. *Proc. Natl. Acad. Sci. USA* 90: 3068–3072.
9. Feske, S., Y. Gwack, M. Prakriya, S. Srikanth, S. H. Puppel, B. Tanasa, P. G. Hogan, R. S. Lewis, M. Daly, and A. Rao. 2006. A mutation in Orai1 causes immune deficiency by abrogating CRAC channel function. *Nature* 441: 179–185.
10. Vig, M., C. Peinelt, A. Beck, D. L. Koomoa, D. Rabah, M. Koblan-Huberson, S. Kraft, H. Turner, A. Fleig, R. Penner, and J. P. Kinet. 2006. CRACM1 is a plasma membrane protein essential for store-operated Ca^{2+} entry. *Science* 312: 1220–1223.
11. Prakriya, M., S. Feske, Y. Gwack, S. Srikanth, A. Rao, and P. G. Hogan. 2006. Orai1 is an essential pore subunit of the CRAC channel. *Nature* 443: 230–233.
12. Yeromin, A. V., S. L. Zhang, W. Jiang, Y. Yu, O. Safrina, and M. D. Cahalan. 2006. Molecular identification of the CRAC channel by altered ion selectivity in a mutant of Orai. *Nature* 443: 226–229.
13. Duffy, S. M., W. J. Lawley, D. Kaur, W. Yang, and P. Bradding. 2003. Inhibition of human mast cell proliferation and survival by tamoxifen in association with ion channel modulation. *J. Allergy Clin. Immunol.* 112: 970–977.
14. Clapham, D. E., L. W. Runnels, and C. Strubing. 2001. The TRP ion channel family. *Nat. Rev. Neurosci.* 2: 387–396.
15. Bradding, P., Y. Okayama, N. Kambe, and H. Saito. 2003. Ion channel gene expression in human lung, skin, and cord blood-derived mast cells. *J. Leukocyte Biol.* 73: 614–620.
16. Nadler, M. J. S., M. C. Hermosura, K. Inabe, A. L. Perraud, Q. Zhu, A. J. Stokes, T. Kurosaki, J. P. Kinet, R. Penner, A. M. Scharenberg, and A. Fleig. 2001. LTRPC7 is a Mg[middot]ATP-regulated divalent cation channel required for cell viability. *Nature* 411: 590–595.

17. Monteilh-Zoller, M. K., M. C. Hermosura, M. J. S. Nadler, A. M. Scharenberg, R. Penner, and A. Fleig. 2002. TRPM7 provides an ion channel mechanism for cellular entry of trace metal ions. *J. Gen. Physiol.* 121: 49–60.
18. Clark, K., M. Langeslag, B. van Leeuwen, L. Ran, A. G. Ryazanov, C. G. Figdor, W. H. Moolenaar, K. Jalink, and F. N. van Leeuwen. 2006. TRPM7, a novel regulator of actomyosin contractility and cell adhesion. *EMBO J.* 25: 290–301.
19. Su, L. T., M. A. Agapito, M. Li, W. T. N. Simonson, A. Huttenlocher, R. Habas, L. Yue, and L. W. Runnels. 2006. TRPM7 regulates cell adhesion by controlling the calcium-dependent protease calpain. *J. Biol. Chem.* 281: 11260–11270.
20. Hanano, T., Y. Hara, J. Shi, H. Morita, C. Umebayashi, E. Mori, H. Sumimoto, Y. Ito, Y. Mori, R. Inoue, et al. 2004. Involvement of TRPM7 in cell growth as a spontaneously activated Ca^{2+} entry pathway in human retinoblastoma cells. *J. Pharmacol. Sci.* 95: 403–419.
21. Sanmugalingam, D., A. J. Wardlaw, and P. Bradding. 2000. Adhesion of human lung mast cells to bronchial epithelium: evidence for a novel carbohydrate-mediated mechanism. *J. Leukocyte Biol.* 68: 38–46.
22. Kirshenbaum, A. S., C. Akin, Y. Wu, M. Rottem, J. P. Goff, M. A. Beaven, V. K. Rao, and D. D. Metcalfe. 2003. Characterization of novel stem cell factor responsive human mast cell lines LAD1 and 2 established from a patient with mast cell sarcoma/leukemia: activation following aggregation of FcεRI or FcγRI. *Leukemia Res.* 27: 677–682.
23. Duffy, S. M., M. L. Leyland, E. C. Conley, and P. Bradding. 2001. Voltage-dependent and calcium-activated ion channels in the human mast cell line HMC-1. *J. Leukocyte Biol.* 70: 233–240.
24. Kraft, R., and C. Harteneck. 2005. The mammalian melastatin-related transient receptor potential cation channels: an overview. *Pflugers Arch. Eur. J. Physiol.* 451: 204–211.
25. Walder, R. Y., D. Landau, P. Meyer, H. Shalev, M. Tsolia, Z. Borochowitz, M. B. Boettger, G. E. Beck, R. K. Englehardt, R. Carmi, and V. C. Sheffield. 2002. Mutation of TRPM6 causes familial hypomagnesemia with secondary hypocalcemia. *Nat. Genet.* 31: 171–174.
26. Schlingmann, K. P., S. Weber, M. Peters, L. Niemann Nejsum, H. Vitzthum, K. Klingel, M. Kratz, E. Haddad, E. Ristoff, D. Dinour, et al. 2002. Hypomagnesemia with secondary hypocalcemia is caused by mutations in TRPM6, a new member of the TRPM gene family. *Nat. Genet.* 31: 166–170.
27. Schmitz, C., A. L. Perraud, C. O. Johnson, K. Inabe, M. K. Smith, R. Penner, T. Kurosaki, A. Fleig, and A. M. Scharenberg. 2003. Regulation of vertebrate cellular Mg^{2+} homeostasis by TRPM7. *Cell* 114: 191–200.
28. Hermosura, M. C., M. K. Monteilh-Zoller, A. M. Scharenberg, R. Penner, and A. Fleig. 2002. Dissociation of the store-operated calcium current I_{CRAC} and the Mg-nucleotide-regulated metal ion current MagNuM. *J. Physiol.* 539: 445–458.
29. Prakriya, M., and R. S. Lewis. 2002. Separation and characterization of currents through store-operated CRAC channels and Mg^{2+}-inhibited cation (MIC) channels. *J. Gen. Physiol.* 119: 487–508.
30. Jiang, X., E. W. Newell, and L. C. Schlichter. 2003. Regulation of a TRPM7-like current in rat brain microglia. *J. Biol. Chem.* 278: 42867–42876.
31. Runnels, L. W., L. Yue, and D. E. Clapham. 2001. TRP-PLIK, a bifunctional protein with kinase and ion channel activities. *Science* 291: 1043–1047.
32. Takezawa, R., C. Schmitz, P. Demeuse, A. M. Scharenberg, R. Penner, and A. Fleig. 2004. Receptor-mediated regulation of the TRPM7 channel through its endogenous protein kinase domain. *Proc. Natl. Acad. Sci. USA* 101: 6009–6014.
33. Schmitz, C., M. V. Dorovkov, X. Zhao, B. J. Davenport, A. G. Ryazanov, and A. L. Perraud. 2005. The channel kinases TRPM6 and TRPM7 are functionally nonredundant. *J. Biol. Chem.* 280: 37763–37771.
34. Duffy, S. M., W. J. Lawley, E. C. Conley, and P. Bradding. 2001. Resting and activation-dependent ion channels in human mast cells. *J. Immunol.* 167: 4261–4270.
35. Duffy, S. M., P. Berger, G. Cruse, W. Yang, S. J. Bolton, and P. Bradding. 2004. The K^+ channel $IK_{Ca}1$ potentiates Ca^{2+} influx and degranulation in human lung mast cells. *J. Allergy Clin. Immunol.* 114: 66–72.
36. Duffy, S. M., G. Cruse, W. J. Lawley, and P. Bradding. 2005. β2-adrenoceptor regulation of the K^+ channel $IK_{Ca}1$ in human mast cells. *FASEB J.* 19: 1006–1008.
37. Sahni, J., B. Nelson, and A. M. Scharenberg. 2007. SLC41A2 encodes a plasma-membrane Mg^{2+} transporter. *Biochem. J.* 401: 505–513.
38. Dorovkov, M. V., and A. G. Ryazanov. 2004. Phosphorylation of Annexin I by TRPM7 channel-kinase. *J. Biol. Chem.* 279: 50643–50646.
39. Alldridge, L. C., and C. E. Bryant. 2003. Annexin 1 regulates cell proliferation by disruption of cell morphology and inhibition of cyclin D1 expression through sustained activation of the ERK1/2 MAPK signal. *Exp. Cell Res.* 290: 93–107.
40. Skouteris, G. G., and C. H. Schroder. 1996. The hepatocyte growth factor receptor kinase-mediated phosphorylation of lipocortin-1 transduces the proliferating signal of the hepatocyte growth factor. *J. Biol. Chem.* 271: 27266–27273.